*Wind and Structures, Vol. 11, No. 5 (2008) 361-376*
DOI: http://dx.doi.org/10.12989/was.2008.11.5.361


# Effect of building volume and opening size on fluctuating internal pressures

John D. Ginger*

*Cyclone Testing Station, James Cook University, Townsville, Queensland, 4811, Australia*

John D. Holmes

*JDH Consulting, Mentone, Victoria, 3194 Australia*

Gregory A. Kopp

*Boundary Layer Wind Tunnel Laboratory, University of Western Ontario, London, N6A 5B9, Canada*

*(Received February 27, 2008, Accepted July 30, 2008)*

**Abstract.** This paper considers internal pressure fluctuations for a range of building volumes and dominant wall opening areas. The study recognizes that the air flow in and out of the dominant opening in the envelope generates Helmholtz resonance, which can amplify the internal pressure fluctuations compared to the external pressure, at the opening. Numerical methods were used to estimate fluctuating standard deviation and peak (i.e. design) internal pressures from full-scale measured external pressures. The ratios of standard deviation and peak internal pressures to the external pressures at a dominant windward wall opening of area, $A_W$ are presented in terms of the non-dimensional opening size to volume parameter, $S^* = (a_s/\overline{U}_h)^2(A_W^{3/2}/V_{Ie})$, where $a_s$ is the speed of sound, $\overline{U}_h$ is the mean wind speed at the top of the building and $V_{Ie}$ is the effective internal volume. The standard deviation of internal pressure exceeds the external pressures at the opening, for $S^*$ greater than about 0.75, showing increasing amplification with increasing $S^*$. The peak internal pressure can be expected to exceed the peak external pressure at the opening by 10% to 50%, for $S^*$ greater than about 5. A dominant leeward wall opening also produces similar fluctuating internal pressure characteristics.

**Keywords:** low-rise building; internal pressure; dominant opening; volume; Helmholtz resonance.

## 1. Introduction

The pressure inside a building, produced by wind action, is dependent on the external surface pressure, the position and size of all openings connecting the exterior to the interior of the building, and the effective volume. The internal pressure in a nominally sealed building is generally small in

* Corresponding Author, E-mail: john.ginger@jcu.edu.au

magnitude compared to external pressures. The porosity of the envelope, $\varepsilon$ (defined as the ratio of effective leakage area to the surface area of the building), of these buildings typically varies between $10^{-4}$ and $10^{-3}$. The failure of a door or window in such a building can create a dominant opening and generate large internal pressures in strong winds. This, in combination with large external pressures acting in the same direction, can result in large net pressures across the envelope. Such a scenario with a dominant windward wall opening, which is a common cause of roof and wall failures in windstorms, is often the governing design criterion.

Liu (1978), Holmes (1979), Vickery (1994) and Harris (1990) were amongst the first to carry out detailed studies on internal pressures in low-rise buildings. They studied internal pressures in nominally sealed buildings with typical porous envelopes, and buildings with large openings in the envelope. In addition, the effects of background leakage and flexibility of the envelope were studied. Since then, Ginger, *et al.* (1997) and Ginger (2000) have carried out full scale studies on internal and net pressures on a full-scale low-rise building, and showed that the results compare favorably with theoretical analysis. Oh, *et al.* (2007) have shown that the same theoretical equations compare satisfactorily with model scale wind tunnel data.

The characteristics of internal pressure fluctuations (and the resulting peak pressure) are influenced by the size of openings in the envelope, the building volume and by the approach wind speed. Holmes (1979, 2008) applied dimensional analysis techniques to describe internal volume scaling requirements that must be satisfied when conducting wind tunnel tests. He showed that in order to correctly simulate internal pressure fluctuations in wind tunnel models, the required scaling ratio for internal volume is the cube of length ratio divided by the velocity ratio squared. If this is not done, the frequencies of internal pressure fluctuations will be scaled incorrectly with respect to those for the external pressures and unreliable results may be obtained. Recent model studies on internal pressure by Oh, *et al.* (2007) and Kopp, *et al.* (2008) have incorporated this volume distortion.

Both model scale and full scale studies have shown that Helmholtz resonance occurs in internal pressure fluctuations in buildings with a dominant opening. The Helmholtz resonant frequency is dependent on the size of the dominant opening and the effective internal volume of the building. Sharma and Richards (2003) indicated that internal pressure resonance can take place at other frequencies in addition to the Helmholtz frequency.

Internal pressure data specified in codes and standards appear to be based on studies from a limited range of dominant opening sizes, effective volumes, and theoretical analyses. In addition, the effects of sizes of the volume and openings in the envelope are either ignored, or are treated very simplistically. In some cases (e.g. ASCE 7-05), a reduction in internal pressure is specified when designing large buildings without due consideration given to the sizes of potential dominant openings. In addition, the "free" volume in some buildings such as those used for bulk material storage, can vary during its operation. Furthermore, there is a possibility that the Helmholtz frequency (or other potential resonance frequencies) could coincide with the natural frequencies of the structural system generating resonant effects that have not been considered in the structural design. Hence, there is a need to analyze the effects of the size of a building volume and the size of openings in its envelope, on the internal pressures generated with respect to a range of (design) wind speeds.

In this paper, characteristics of internal pressures in typical buildings, with a range of dominant opening sizes and volumes, are studied using available full-scale data. Particular attention is paid to Helmholtz frequencies, and to assessment of the effect of the approach wind speed on internal pressure. The results will be useful for determining the importance of the sizes of dominant opening area and building volume when calculating design internal pressures. They are presented in a non-dimensional format useful for design standards.

Internal pressures are simulated in buildings with a range of volumes and opening sizes, for measured external pressure fluctuations at the dominant windward wall opening, and also compared with available experimental data. Simulated internal to measured windward wall external, standard deviation and peak (i.e. maximum) pressure ratios and gain functions, are calculated for these building configurations. These results provide quantitative assessments of internal pressure characteristics, and amplification or attenuation of internal pressure compared to external pressure fluctuations at the dominant windward wall opening. In addition, simulated internal to measured leeward wall external, standard deviation and peak (i.e. minimum) pressure ratios are also presented for a range of building volumes and dominant leeward wall opening sizes.

## 2. Theory

The mean, standard deviation and peak (i.e. maximum and minimum), external pressures ($p_E$) and internal pressures ($p_I$) are defined in coefficient form as:

$$C_{\bar{p}} = \frac{\bar{p}}{\frac{1}{2}\rho \bar{U}_h^2}, \; C_{\sigma p} = \frac{\sigma_p}{\frac{1}{2}\rho \bar{U}_h^2}, \; C_{\hat{p}} = \frac{\hat{p}}{\frac{1}{2}\rho \bar{U}_h^2} \text{ and } C_{\breve{p}} = \frac{\breve{p}}{\frac{1}{2}\rho \bar{U}_h^2}$$

where,

$\bar{p}$, $\sigma_p$, $\hat{p}$, $\breve{p}$ are the mean, standard deviation, maximum and minimum pressures
$\rho$ is the density of air, and
$\bar{U}_h$ is the mean wind speed at roof height, $h$

Pressures acting towards a surface are defined as positive. The characteristics (i.e. frequency distribution) of pressure fluctuations are further studied by analyzing their spectral densities, given by *S(f)*. Assuming linearity, the internal pressure fluctuations can be related to the external pressures using the frequency dependent admittance function, $|\chi_{p_I/p_E}|^2$ shown in Eqs. (1a-b). This admittance function is also defined as square of the gain function $G(f)^2$.

$$S_{p_I}(f) = |\chi_{p_I/p_E}|^2 S_{p_E}(f) \tag{1a}$$

$$G(f)^2 = |\chi_{p_I/p_E}|^2 \tag{1b}$$

The relationship between peak (i.e. maximum and minimum), mean and standard deviation pressures can be described by the pressure peak factor, $g_p$ where $C_{\hat{p}}$, $C_{\breve{p}} = C_{\bar{p}} \pm g_p C_{\sigma p}$. In the case of external pressures, the pressure peak factor $g_p$ typically ranges from about 4 to 5 depending on the location of the building and the extent over which the pressure is acting and the level of turbulence in the flow.

### 2.1. Mean internal pressure

Liu (1978) used the principle of conservation of mass in a building and steady flow through a windward opening area $A_W$ and a leeward opening area $A_L$, to obtain the relationship between mean internal pressure ($\bar{p}_I$), mean external windward pressure ($\bar{p}_W$) and mean external leeward pressure ($\bar{p}_L$), by Eq. (2). This relationship is used in many codes and standards (i.e. AS/NZS 1170.2; Standards Australia, 2002) to derive quasi-steady internal pressure coefficients for given $A_W/A_L$ ratios, in buildings. Results from wind tunnel model scale and full scale studies (Holmes 1979, Ginger, *et al.* 1997) have shown that the mean internal pressures can be satisfactorily estimated using Eq. (2). For a building with a single opening, Eq. (2) shows that the mean internal pressure is equal to the mean external pressure at the opening. Furthermore, when the size of an opening is greater than about thrice the total background leakage, the mean external pressures at the opening and on rest of the building, will influence the mean internal pressure at a ratio of about 9:1.

$$C_{\bar{p}_I} = \frac{C_{\bar{p}_W}}{1+(A_L/A_W)^2} + \frac{C_{\bar{p}_L}}{1+(A_W/A_L)^2} \tag{2}$$

Although the limiting case of a dominant opening is that of a building with a single opening, Vickery (1994) showed that the internal pressure fluctuations are not significantly influenced if the total background leakage area is less than about 10% of the dominant opening. In such cases, a reasonable approach is to study the pressure in a sealed building with a single opening.

### *2.2. Fluctuating internal pressure – (Building containing a dominant opening)*

Holmes (1979) derived Eq. (3), to describe the time dependent internal pressure in a building with a dominant opening of area $A$, in terms of internal pressure coefficient, $C_{p_I}$ and external pressure coefficient at the opening, $C_{p_E}$. Here, $p_0$ is the atmospheric pressure, $k$ is the discharge coefficient of the opening, $n$ is the ratio of specific heats of air and $l_e = \sqrt{(\pi A/4)}$ is the effective length of the "slug" of air moving in and out of the opening. Vickery (1994) showed that the effect of building flexibility on internal pressure fluctuations can be accounted for by the use of an effective internal volume $V_{Ie}$ (the actual "free" volume increased by a factor, $K_A/K_B$, where, $K_A$ is the bulk modulus of air and $K_B$ is the bulk modulus of the building). The speed of sound $a_s = (n \times p_0/\rho)^{1/2}$, where $n = 1.4$ for an adiabatic process.

$$\frac{\rho l_e V_{Ie}}{nAp_0}\ddot{C}_{p_I} + \left[\frac{\rho V_{Ie}\bar{U}_h}{2nkAp_0}\right]^2 \dot{C}_{p_I}\left|\dot{C}_{p_I}\right| + C_{p_I} = C_{p_E} \tag{3}$$

The first term in Eq. (3) describes the "inertia" of the air flow in and out of the opening, while the second term represents the damping of the flow through the opening. The undamped Helmholtz frequency is

$$f_H = \frac{1}{2\pi}\sqrt{\frac{nAp_0}{\rho l_e V_{Ie}}} \tag{4}$$

Eq. (3) shows that the damping is reduced as the ratio of opening area to internal volume is increased. However, by Eq. (4) this will increase the Helmholtz frequency, and hence its overall effect on internal pressure fluctuations is not easily determined. This is because the characteristics of the internal pressure fluctuations will depend on the spectral density of the external pressure fluctuations at the opening and the Helmholtz frequency. If the Helmholtz frequency falls in the energy containing range of external pressure fluctuations (i.e. less than 1Hz), and conditions are such that damping is small, then the internal pressures could be amplified, compared to the external pressure fluctuations at the opening.

Model scale studies by Sharma and Richards (2003) described the possible occurrence of self-sustaining vortex driven resonance inside a building when the opening in the wall is generally parallel to the approach flow. They also noted that these resonant effects could significantly increase the fluctuating component of internal pressure. In this case, this secondary resonant frequency was found to be a function of the approach wind speed and size of the opening.

### 2.2.1. Numerical analysis

Internal pressures can be simulated for a range of internal volumes, $V_{Ie}$ and dominant opening areas, $A$ using the measured external pressure fluctuations at the opening by applying a first order explicit finite difference scheme to solve Eq. (3). The time derivatives of internal pressures are calculated at each time step $j$, based on $C_{pI}$ values at the preceding two time steps, as shown in Eq. (5), where $\Delta t$ is the time step. In these simulations, the measured mean wind speed and atmospheric pressure $p_0$, are used, along with the external pressure coefficient $C_{pE}$ values measured at each time step as the driving function.

$$\dot{C}_{p_I}^{(j)} = \frac{C_{p_I}^{(j)} - C_{p_I}^{(j-1)}}{\Delta t} \text{ and } \ddot{C}_{p_I}^{(j)} = \frac{C_{p_I}^{(j)} - 2C_{p_I}^{(j-1)} + C_{p_I}^{(j-2)}}{\Delta t^2} \tag{5}$$

## 2.3. Dimensional analysis for internal pressure fluctuations

Holmes (1979) showed that the internal pressure fluctuations can be represented as a function of the five non-dimensional parameters shown in Eq. (6).

$$C_{\sigma_{pI}} = f(\Phi_1, \Phi_2, \Phi_3, \Phi_4, \Phi_5) \tag{6}$$

where, $\Phi_1 = \frac{A^{\frac{3}{2}}}{V_{Ie}}$, $\Phi_2 = \frac{a_s}{\bar{U}_h}$, $\Phi_3 = \frac{\rho \bar{U}_h \sqrt{A}}{\mu}$, $\Phi_4 = \frac{\sigma_U}{\bar{U}}$, $\Phi_5 = \frac{\lambda_U}{\sqrt{A}}$

and $\mu$ is the viscosity of air, $\bar{U}$ and $\sigma_U$ are the mean velocity and turbulence intensity respectively of the flow at a given elevation, and $\lambda_U$ is the integral length scale of turbulence.

The Reynolds No. term, $\Phi_3$, which in most cases cannot be matched in typical small scale model studies, is not likely to be an important parameter except for small opening areas, $A$. As this study focuses on large dominant openings, such a mismatch is not considered to be critical.

Eq. (3) can be written in the non-dimensional form of Eq. (7), by introducing the non-dimensional parameters given in Eq. (6), and by defining a non-dimensional time, $t^* = \frac{t\bar{U}_h}{\lambda_U}$.

$$\left(\frac{\sqrt{\pi}}{2}\right)\frac{1}{\Phi_1\Phi_2^2\Phi_5^2}\frac{d^2C_{p_I}}{dt^{*2}} + \left(\frac{1}{4k^2}\right)\left[\frac{1}{\Phi_1\Phi_2^2\Phi_5}\right]^2\frac{dC_{p_I}}{dt^*}\left|\frac{dC_{p_I}}{dt^*}\right| + C_{p_I} = C_{p_E} \tag{7}$$

The product $\Phi_1\Phi_2^2$ in Eq. (7), can be replaced by a single non-dimensional variable and defined as the non-dimensional opening size to volume parameter, $S^* = (a_s/\bar{U}_h)^2(A^{3/2}/V_{Ie})$. Eq. (7) shows that the variation of internal pressure for given external pressure fluctuations (i.e. the forcing function $C_{pE}$) is dependent on $S^*$, $\Phi_5$ and $k$, and that there is a unique solution for $C_{pI}$ with $S^*$, for a given $\Phi_5$ and $k$. Therefore, given the value of $k$, the ratio of internal pressure fluctuations to external pressure fluctuations at the opening, can be presented by a family of curves, with variables of $S^*$ and $\Phi_5$.

Holmes (1979) also applied dimensional analysis methods to show that the internal volume of a model building must be distorted in order to correctly simulate internal pressure fluctuations, at model scale. The same rules were derived by Holmes (2008) using alternative non-dimensional parameters based on matching Helmholtz frequency (in buildings with a dominant opening), or the characteristic frequency (in permeable buildings) with the frequencies in the approach turbulent flow.

The Helmholtz frequency is: $f_H \propto \sqrt{\frac{\sqrt{A}p_0}{\rho V_{Ie}}}$; $f_H^2 \propto \sqrt{\frac{\sqrt{A}.p_0}{\rho V_{Ie}}}$

For wind tunnel testing at normal atmospheric pressures and differing test velocities, the ratio of model to full-scale frequency is given by:

$$[f_H^2]_r = \frac{[L]_r[p_0]_r}{[\rho]_r[V_{Ie}]_r} = \frac{[L]_r}{[V_{Ie}]_r}$$

since the ratios $[p_0]_r = 1.0$ and $[\rho]_r = 1.0$, for tests carried out at normal pressures in air. (The subscript $r$ denotes the model to full scale ratio).

The approach flow frequency scaling requires that: $[f]_r = \frac{[U]_r}{[L]_r}$

Hence, for correct frequency scaling, $\frac{[L]_r}{[V_{Ie}]_r} = \frac{[U^2]_r}{[L^2]_r}$

Thus, the internal volume of a building should be scaled according to the relationship $[V_{Ie}]_r = [L^3]_r/[U^2]_r$. Holmes (2008) also derived the same scaling relationship for permeable buildings. This indicates that the volume (of the model or the full-scale building) must be distorted by a factor $1/[U^2]_r$ to maintain similarity, and obtain reliable internal pressure measurements. Eq. (7) also shows similarity is maintained by keeping $S^*$ constant, which gives these same volume distortion requirements.

## 3. Experimental data and analysis

The analysis in this paper is based on external and internal pressure fluctuations measured on the 13.7×9.1×4.0 m Texas Tech full-scale test building, shown in Fig. 1. The effective volume of the building $V_{Ie}$ was estimated by Ginger (2000) as 1175 m$^3$. The approach terrain can be classified as Category 2 according to AS/NZS1170.2, the topography is flat, and the turbulence intensity $\sigma_U/\bar{U}$, at roof height of 4m, is about 0.20. External pressures ($p_E$) and internal pressure ($p_I$) measured during strong winds were low-pass filtered at 8 Hz, and sampled at 40 Hz for a single run of 15 mins duration. The velocity was sampled at 10 Hz. The results were obtained when $\bar{U}_h$ exceeds 7 m/s. The longitudinal integral scale $\lambda_U$ at the roof height of 4 m was estimated by Levitan and Mehta (1992) to be 107 m

External pressures measured at tap locations 11407 or 31407 on the center of the wall, and

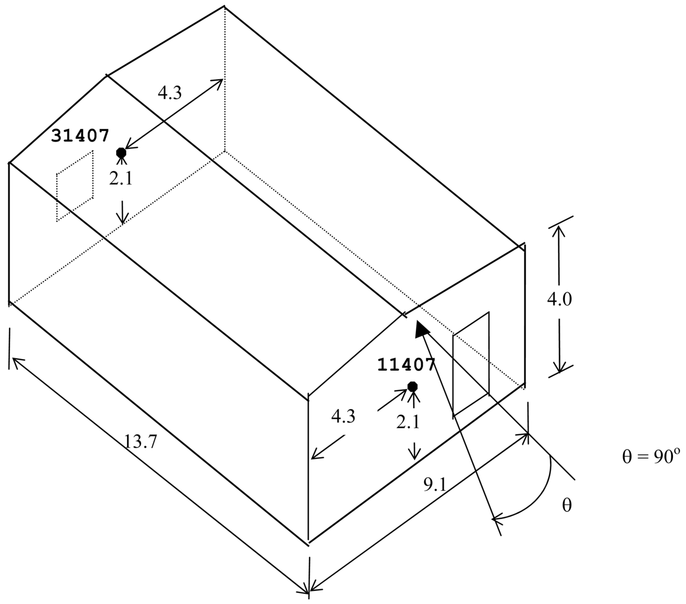


Fig. 1 13.7×9.1×4.0 m full scale test building at Texas Tech Tap Locations • All dimensions in m

Table 1a Mean, standard deviation, and maximum windward wall external andinternal pressure coefficients on the Texas Tech Test building with a dominant windward wall opening

| $A_W$ (m$^2$) | $C_{\bar{p}_E}$ | $C_{\sigma_{pE}}$ | $C_{\hat{p}_E}$ | $C_{\bar{p}_I}$ | $C_{\sigma_{pI}}$ | $C_{\hat{p}_I}$ | $S^*$ | $\sigma_{pI}/\sigma_{pE}$ | $g_{pI}$ | $\hat{p}_I/\hat{p}_E$ |
|---|---|---|---|---|---|---|---|---|---|---|
| 0.4 | 0.63 | 0.32 | 2.35 | 0.60 | 0.30 | 2.25 | 0.4 | 0.9 | 5.5 | 0.96 |
| 0.8 | 0.62 | 0.42 | 2.76 | 0.61 | 0.42 | 2.74 | 1.4 | 1.0 | 5.1 | 0.99 |
| 2.0 | 0.60 | 0.31 | 2.28 | 0.60 | 0.31 | 2.20 | 5.0 | 1.0 | 5.2 | 0.96 |

Table 1b Mean, standard deviation, and minimum leeward wall external and internal pressure coefficients on the Texas Tech Test building with a dominant leeward wall opening

| $A_L$ (m$^2$) | $C_{\bar{p}_E}$ | $C_{\sigma_{pE}}$ | $C_{\breve{p}_E}$ | $C_{\bar{p}_I}$ | $C_{\sigma_{pI}}$ | $C_{\breve{p}_I}$ | $S^*$ | $\sigma_{pI}/\sigma_{pE}$ | $g_{pI}$ | $\breve{p}_I/\breve{p}_E$ |
|---|---|---|---|---|---|---|---|---|---|---|
| 2.0 | -0.35 | 0.11 | -0.78 | -0.35 | 0.10 | -0.82 | 5.0 | 0.9 | 4.7 | 1.04 |

internal pressure measured within the building shown in Fig. 1, are used in this study. Data obtained for wind orientations (θ) of 90° ± 10°, and 270° ± 10° (i.e. wind flow perpendicular to the 9.1 m sides of building) with a single windward wall opening $A_W$ of 0.4, 0.8 or 2.0 m$^2$ (i.e. 1%, 2% and 5% of wall area), and a single leeward wall opening $A_L$ of 2.0 m$^2$ (i.e. 5% of wall area), in addition to background leakage (porosity, $\varepsilon \sim 3\times10^{-4}$), are presented in this paper.

The measured windward wall external and internal mean, standard deviation and peak (i.e. maximum) pressure coefficients and the internal pressure peak factors on the building with a 1%, 2% or 5% windward wall opening ($A_W$ = 0.4, 0.8 or 2.0 m$^2$ respectively) at $S^* \sim 0.4$, 1.4 and 5 are shown in Table 1a. The measured leeward wall external and internal mean, standard deviation and peak (i.e. minimum) pressure coefficients and the internal pressure peak factors on the building with a 5% leeward wall opening ($A_L = 2.0\ \text{m}^2$) at $S^* \sim 5$ are shown in Table 1b. The ratios of internal to external standard deviation and peak pressures also listed in Tables 1a and 1b, show that the fluctuating and peak pressures are of similar magnitude, for these cases.

The measured windward wall external pressure spectra, internal pressure spectra (with a dominant windward wall opening) and internal-external pressure admittance functions are shown in Figs. 2(a-c). The measured internal pressure spectra and admittance functions show that internal pressure resonance occurs close to the calculated Helmholtz frequencies of 1.3 Hz, 1.6 Hz and 2.0 Hz, for the open areas of 0.4, 0.8 and $2.0\ \text{m}^2$, respectively. Ginger, *et al.* (1995) showed that internal pressure Helmholtz resonance also occurs in the building with a dominant leeward wall opening. However, as the

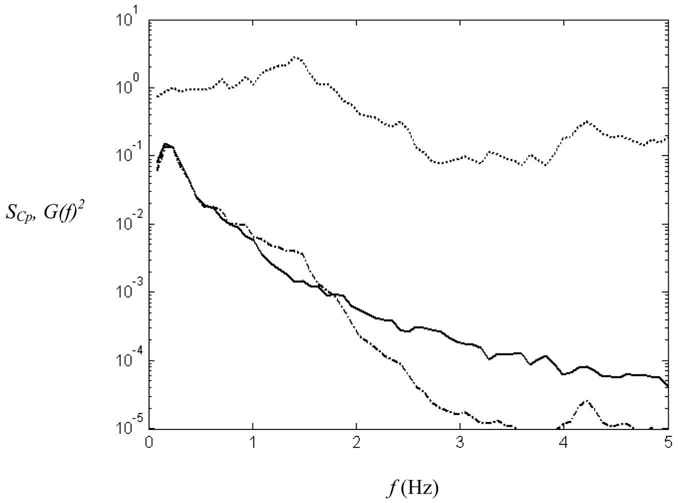


Fig. 2(a) Measured $S_{CpE}$ (—), $S_{CpI}$ (- . - . -.), and $G(f)^2$ (·······) *vs* $f$ $A_W = 1\%$

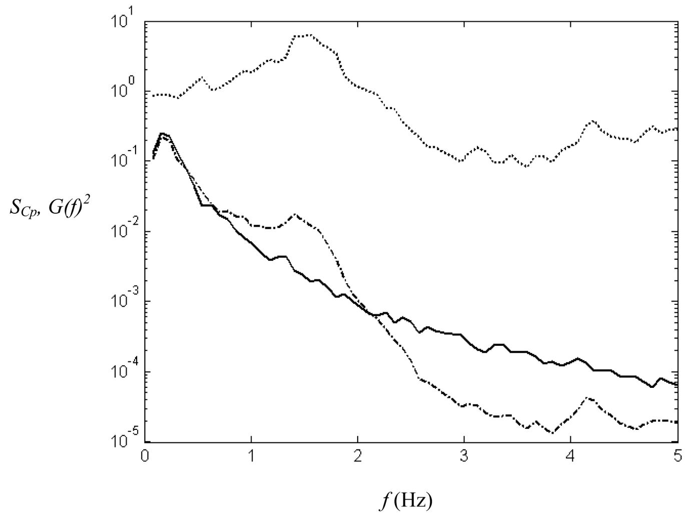


Fig. 2(b) Measured $S_{CpE}$ (—), $S_{CpI}$ (- . - . -.), and $G(f)^2$ (·······) *vs* $f$ $A_W = 2\%$

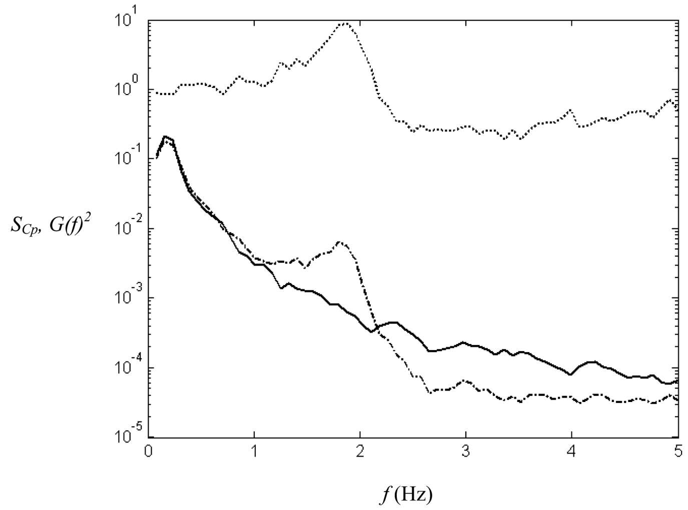


Fig. 2(c) Measured $S_{CpE}$ ( — ), $S_{CpI}$ (- . - . - .), and $G(f)^2$ (⋯⋯) *vs f* $A_W = 5\%$

Helmholtz frequencies are outside the high energy content region of the external pressure spectra (i.e. greater than 1 Hz), the peak and standard deviation internal to external pressure ratios are close to 1.0.

## 4. Results and discussion

The admittance functions $G(f)^2$ and pressure spectra $S_p(f)$ obtained from measured windward wall external pressure and simulated internal pressures (using $k = 0.6$) for $\Phi_5 = 100$, 50, 20 and 10, and $S^* = (a_s/\overline{U}_h)^2(A_W^{3/2}/V_{Ie})$ of 0.014, 0.14, 1.4 and 14 are shown in Figs. 3(a-d), respectively.

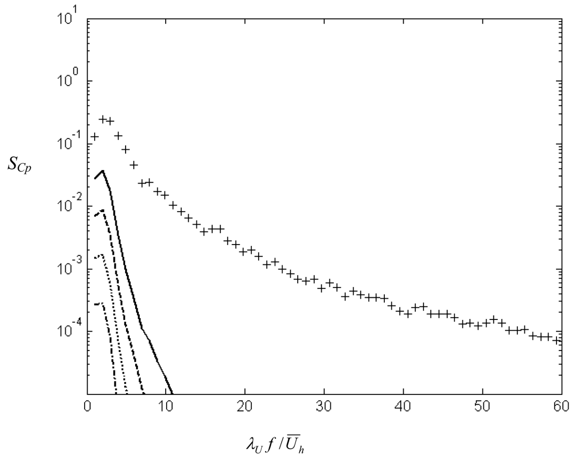


Fig. 3(a) Measured $S_{CpE}$ ( + + + + ), and simulated $S_{CpI}$, $\Phi_5 = 100$ (——), $\Phi_5 = 50$ (- - - -), $\Phi_5 = 20$ (........), $\Phi_5 = 10$ (- . - . - .) dominant windward wall opening, $S^* = 1.4\times10^{-2}$

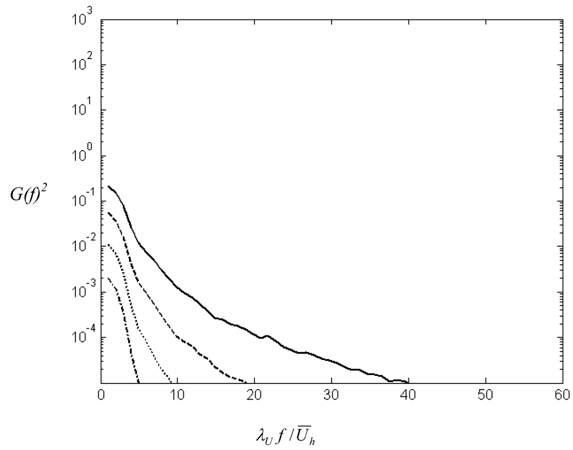


Fig, 3(a) (cont) Simulated internal - external pressure admittance function $\Phi_5 = 100$ (——), $\Phi_5 = 50$ (- - - -), $\Phi_5 = 20$ (........), $\Phi_5 = 10$ (- . - . - .) dominant windward wall opening, $S^* = 1.4\times10^{-2}$

The figures show that internal pressure resonance occurs at the Helmholtz frequency. According to Eq. (7), a reduction in $\Phi_5$ for a given $S^*$ results in increased damping of internal pressure fluctuations and lower peaks in $G(f)^2$ near the Helmholtz frequency. In addition, the non-dimensional Helmholtz frequency is reduced. Figs. 3(c) and 3(d) show that for $S^* > 1.4$, a decrease in $\Phi_5$ tends to move the Helmholtz frequency towards the energy containing range of frequencies, and hence increases the pressure fluctuations, notwithstanding an increase in damping. Figs. 3(a) and 3(b) show that for $S^* < 0.14$, a decrease in $\Phi_5$ tends to move the Helmholtz frequency towards the lower energy range of frequencies, and hence decreases the pressure fluctuations, in combination

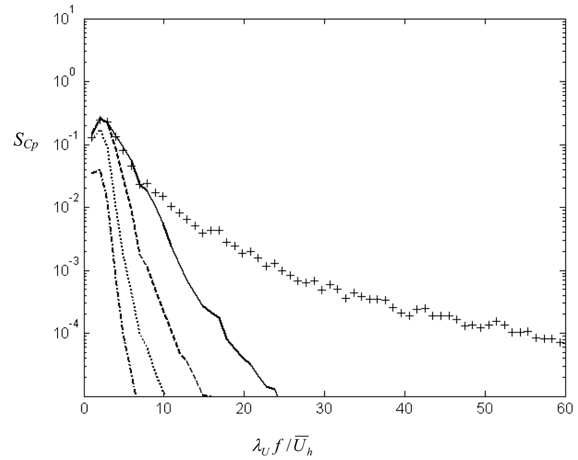


Fig. 3(b) Measured $S_{CpE}$ (+ + + +), and simulated $S_{CpI}$, $\Phi_5 = 100$ (——), $\Phi_5 = 50$ (- - - -), $\Phi_5 = 20$ (……..), $\Phi_5 = 10$ (- . - . - .) dominant wind ward wall opening, $S^* = 1.4\times10^{-1}$

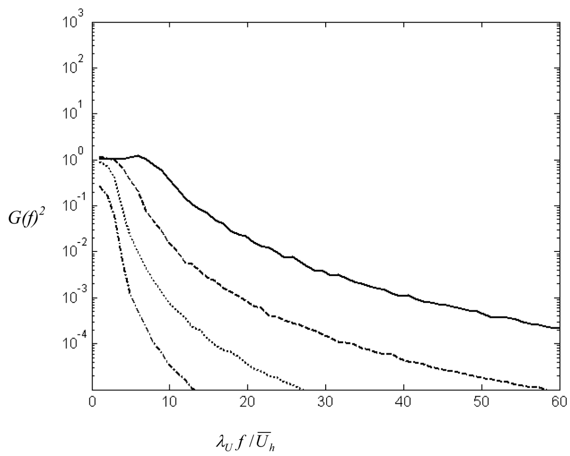


Fig. 3(b) (cont) Simulated internal - external pressure admittance function $\Phi_5 = 100$ (——), $\Phi_5 = 50$ (- - - -), $\Phi_5 = 20$ (……..), $\Phi_5 = 10$ (- . - . - .) dominant windward wall opening, $S^* = 1.4\times10^{-1}$

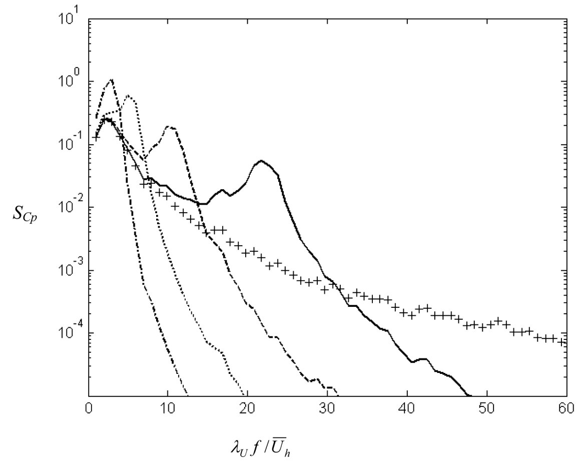


Fig. 3(c) Measured $S_{CpE}$(+ + + +), and simulated $S_{CpI}$, $\Phi_5 = 100$ (——), $\Phi_5 = 50$ (- - - -), $\Phi_5 = 20$ (……..), $\Phi_5 = 10$ (- . - . - .) dominant wind ward wall opening, $S^* = 1.4\times10^{0}$

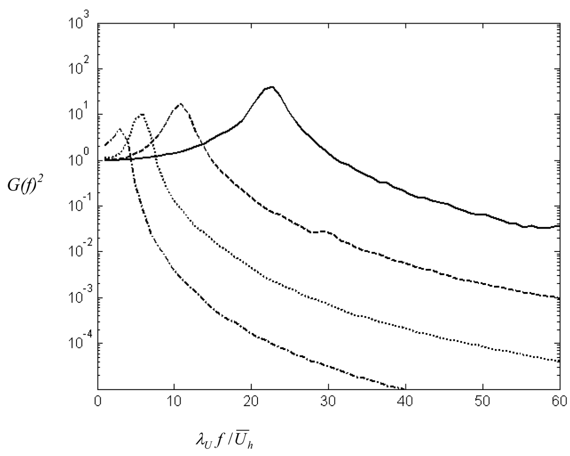


Fig. 3(c) (cont) Simulated internal - external pressure admittance function $\Phi_5 = 100$ (——), $\Phi_5 = 50$ (- - - -), $\Phi_5 = 20$ (……..), $\Phi_5 = 10$ (- . - . - .) dominant windward wall opening, $S^* = 1.4\times10^{0}$

with an increase in damping. As evident from Eq. (7), at these smaller $S^*$ values, the resonance is damped and the internal pressure spectra tend to resemble those in a building without openings, as described by Ginger (2000).

Standard deviation and peak (i.e. maximum), simulated internal to measured windward wall external pressure ratios are shown for $\Phi_5 = 100$, 50, 20 and 10, ($k = 0.6$) as a function $S^* = (a_s/\bar{U}_h)^2(A_W^{3/2}/V_{Ie})$, in Figs. 4 and 5 respectively. The measured internal to measured windward wall external, standard deviation and peak pressure ratios also shown in these figures are for $A_W = 0.4$, 0.8 and 2.0 m$^2$ ($S^* \sim 0.4$, 1.4 and 5, and $\Phi_5 = 169$, 119, 75) respectively. This analysis shows that the size of the opening and volume play an important part in internal pressure fluctuations. The magnitude of the internal pressure standard deviation exceeds that of the external pressure standard deviation at the opening, when $S^*$ is greater than about 0.75. For a given $S^*$ greater than 0.75, an increase in $A_W$ results in further amplification of internal pressure fluctuations. Internal pressure fluctuations are lower than the external pressure fluctuations at the opening, when

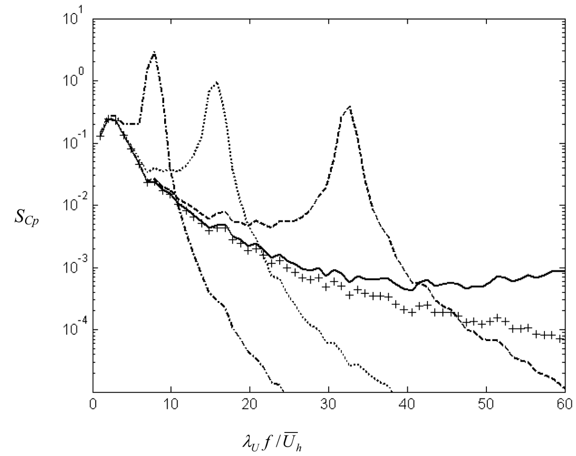


Fig. 3(d) Measured $S_{CpE}$ (+ + + +), and simulated $S_{CpI}$, $\Phi_5 = 100$ (——), $\Phi_5 = 50$ (- - - -), $\Phi_5 = 20$ (……..), $\Phi_5 = 10$ (- . - . - .) dominant wind ward wall opening, $S^* = 1.4\times10^1$

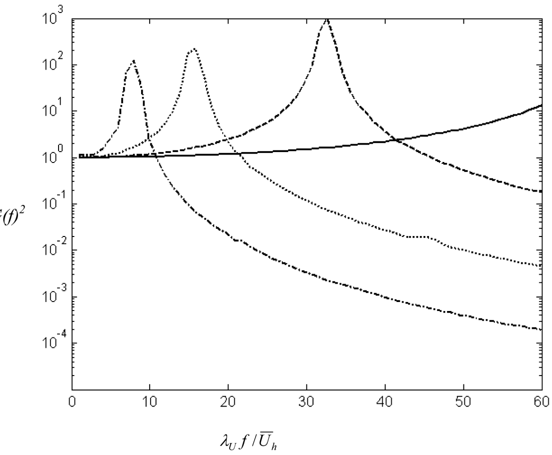


Fig. 3(d) (cont) Simulated internal - external pressure admittance function $\Phi_5 = 100$ (——), $\Phi_5 = 50$ (- - - -), $\Phi_5 = 20$ (……..), $\Phi_5 = 10$ (- . - . - .) dominant windward wall opening, $S^* = 1.4 \times10^1$

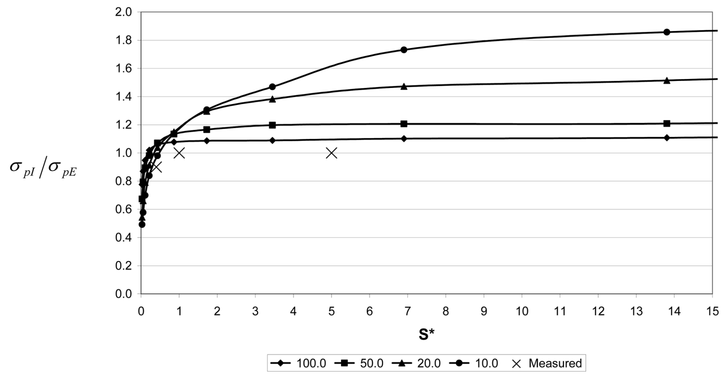


Fig. 4 $\sigma_{pI}/\sigma_{pE}$ vs $S^*$ with a dominant windward wall opening simulated with $k = 0.6$, $\Phi_5 = 100$, 50, 20 and 10

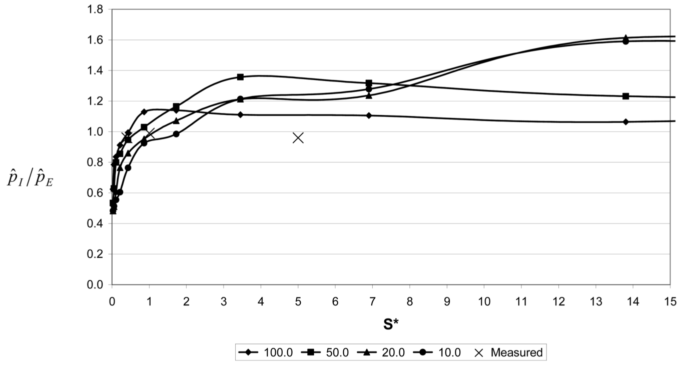


Fig. 5 $\hat{p}_I/\hat{p}_E$ vs $S^*$ with a dominant windward wall opening simulated with $k = 0.6$, $\Phi_5 = 100$, 50, 20 and 10

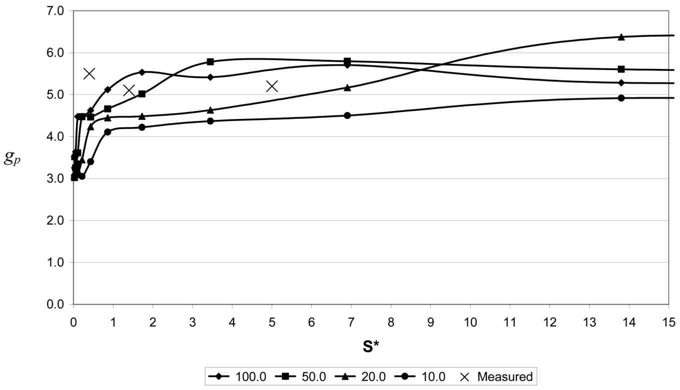


Fig. 6 $g_{pI}$ vs $S^*$ with a dominant windward wall opening simulated with $k = 0.6$, $\Phi_5 = 100$, 50, 20 and 10

$S^*$ is less than about 0.2, especially with increasing $A_W$. Yu, *et al.* (2006) carried out a parametric study on buildings with a dominant opening and found similar relationships. However, the ratio of internal to external pressure fluctuations that they derived, for varying volumes are not unique, and hence cannot be applied universally.

The magnitude of peak internal pressure compared to the peak external pressure at the opening is more variable. The peak internal pressure is expected to exceed the peak external pressure at the opening for $S^*$ larger than about 0.5, 0.8, 1.0 and 2.0 for $\Phi_5 = 100$, 50, 20 and 10, respectively. Furthermore, the peak internal pressure can exceed the external pressure by more than 10% of the peak external pressure, for large values of $S^*$.

The variation of internal pressure peak factor $g_p$ with $S^*$ is shown in Fig. 6. The internal pressure peak factor $g_p$ increases from about 3.0 to 5.0 or more with increasing $S^*$. Furthermore, increasing values of $\Phi_5$ result in larger increases in $g_p$ for $S^*$ larger than about 2, indicating the reduced effect of damping. This is consistent with the increasing influence of Helmholtz resonance which amplifies the internal pressure standard deviations with increasing $S^*$.

The measured data also show similar characteristics, albeit with a lower amplification, indicating possibly that background leakage contributes to effectively increase damping in the internal pressure fluctuations. Model and full scale studies (Holmes, 1979. Ginger, *et al.* 1997) have also shown that a smaller $k$ (in the range of 0.15 to 0.4) may be more appropriate under highly fluctuating turbulent

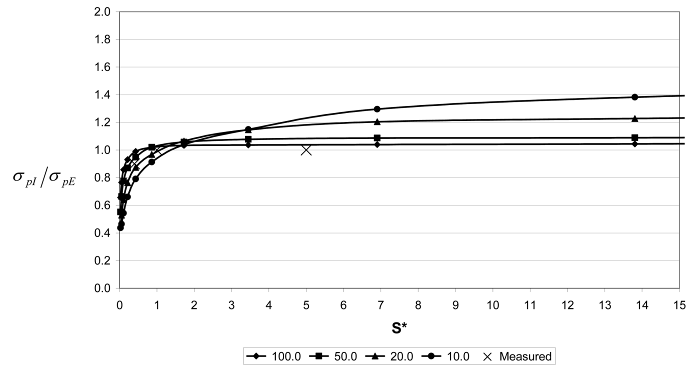


Fig. 7 $\sigma_{pI}/\sigma_{pE}$ vs $S^*$ with a dominant windward wall opening, simulated with $k = 0.3$, $\Phi_5 = 100$, 50, 20 and 10

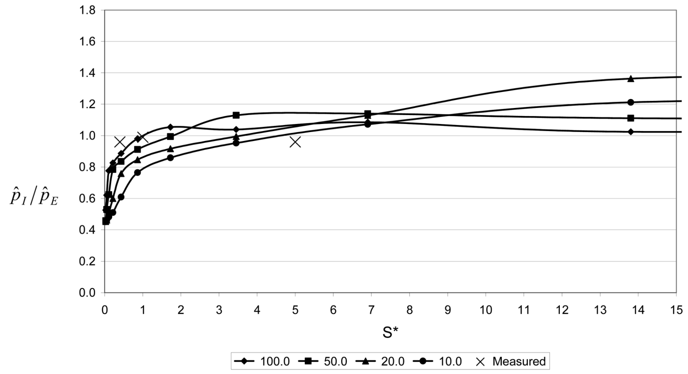


Fig. 8 $\hat{p}_I/\hat{p}_E$ vs $S^*$ with a dominant windward wall opening, simulated with $k = 0.3$, $\Phi_5 = 100$, 50, 20 and 10

flows moving in and out of an opening. As shown in Eq. (7), a smaller $k$ will increase damping and result in lower Helmholtz resonance peaks and hence lower internal pressure standard deviations and peaks for a given $S^*$. Standard deviation and peak, internal to windward wall external pressure ratios are shown for $\Phi_5 = 100$, 50, 20 and 10, ($k = 0.3$) as a function $S^* = (a_s/\bar{U}_h)^2(A_W^{3/2}/V_{Ie})$, in Figs. 7 and 8 respectively. These figures show that the relationship between internal and windward wall external pressure fluctuations have similar trends (as for $k = 0.6$) albeit with lower internal pressure fluctuations as a result of increased damping. Nevertheless, the peak internal pressure can be expected to exceed the peak external pressure when $S^*$ exceeds about 2 for $\Phi_5$ higher than 50, and when $S^*$ exceeds about 5 for $\Phi_5$ lower than 10. This result is in sharp contrast to the rules of codes and standards, which ignore the amplification effects of Helmholtz resonance.

Table 2 gives the internal pressures in buildings with a range of internal volumes and dominant windward wall openings, subjected to typical design wind speeds. The buildings are categorized according to their volumes $V_{Ie}$. Table 2, also shows the estimated Helmholtz frequencies along with the ratios of internal to external standard deviation and peak pressures extracted from Figs. 4 and 5, (derived from applying $k = 0.6$ in the simulations) and Figs. 7 and 8, (derived from applying $k = 0.3$ in the simulations). Based on the discussions in Vickery (1994), these internal to external fluctuating pressure ratios are appropriate for buildings where the total background leakage is less than 10% of the dominant opening area, $A_W$ of each case.

Standard deviation and peak (i.e. minimum) simulated internal to leeward wall external pressure

Table 2 Estimated internal to external pressure standard deviations and peak ratios for buildings with a dominant windward wall opening

| $V_{Ie}$ (m$^3$) | $\overline{U}_h$ (m/s) | $A_W$ (m$^2$) | $f_H$ (Hz) | $S^*$ | $\Phi_5$ | $\sigma_{pI}/\sigma_{pE}$ $k$ = 0.6 | $\sigma_{pI}/\sigma_{pE}$ $k$ = 0.3 | $\breve{p}_I/\breve{p}_E$ $k$ = 0.6 | $\breve{p}_I/\breve{p}_E$ $k$ = 0.3 |
|---|---|---|---|---|---|---|---|---|---|
| | | 0.1 | 2.3 | 0.05 | 338 | 0.8 | 0.7 | 0.7 | 0.5 |
| 200 | 20 | 1 | 4.1 | 1.5 | 107 | 1.1 | 1.0 | 1.1 | 1.0 |
| | | 5 | 6.1 | 16 | 48 | 1.2 | 1.1 | 1.2 | 1.1 |
| | | 1 | 1.3 | 0.14 | 107 | 1.0 | 0.8 | 0.9 | 0.8 |
| 2000 | 20 | 10 | 2.3 | 4.5 | 33 | 1.3 | 1.1 | 1.3 | 1.1 |
| | | 25 | 2.9 | 18 | 21 | 1.5 | 1.2 | 1.6 | 1.4 |
| | | 1 | 0.6 | 0.01 | 107 | 0.7 | 0.5 | 0.6 | 0.6 |
| 10000 | 30 | 10 | 1.0 | 0.41 | 33 | 1.0 | 0.9 | 0.8 | 0.9 |
| | | 40 | 1.4 | 3.3 | 17 | 1.4 | 1.1 | 1.2 | 1.0 |
| | | 10 | 0.7 | 0.46 | 33 | 1.1 | 0.9 | 0.8 | 0.8 |
| 20000 | 20 | 40 | 1.0 | 3.6 | 17 | 1.4 | 1.2 | 1.1 | 1.0 |
| | | 80 | 1.2 | 10 | 12 | 1.8 | 1.3 | 1.5 | 1.2 |
| | | 10 | 0.3 | 0.04 | 33 | 0.7 | 0.5 | 0.5 | 0.5 |
| 100000 | 30 | 40 | 0.5 | 0.33 | 17 | 0.9 | 0.8 | 0.8 | 0.7 |
| | | 100 | 0.6 | 1.3 | 11 | 1.1 | 1.0 | 0.9 | 0.8 |

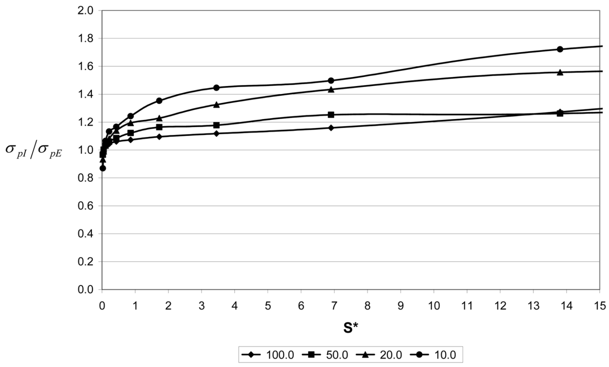


Fig. 9 $\sigma_{pI}/\sigma_{pE}$ vs $S^*$ with a dominant leeward wall opening, simulated with $k$ = 0.6, $\Phi_5$ = 100, 50, 20 and 10

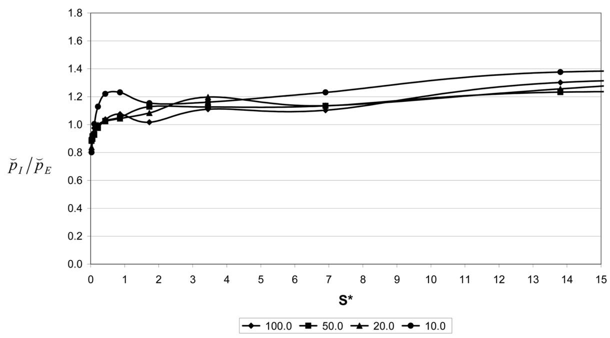


Fig. 10 $\breve{p}_I/\breve{p}_E$ vs $S^*$ with a dominant leeward wall opening, simulated with $k$ = 0.6, $\Phi_5$ = 100, 50, 20 and 10 ratios are shown for $\Phi_5 = 100$, 50, 20 and 10, ($k = 0.6$) as a function $S^* = (a_s/\bar{U}_h)^2(A_L^{3/2}/V_{Ie})$, in Figs. 9 and 10 respectively. These figures for a building with a dominant leeward wall opening show that the relationship between internal and leeward wall external pressure have similar trends as for the building with a dominant windward wall opening (see Figs. 5 and 6), notwithstanding its lesser importance to building design. Ginger, *et al.* (1997) also showed that the pressure fluctuations on the roof and side walls are generally spread over higher frequencies than those on the windward wall, and hence a dominant opening in these areas will to have a greater influence from Helmholtz resonance and possibly generate increased internal pressure fluctuations.

ASCE 7 (American Society of Civil Engineers, 2005) has adopted a reduction factor for peak internal pressures (Eq. 6.16 in ASCE 7-05) that depends on internal volume and opening area. This is always less than 1.0, apparently because the effects of Helmholtz resonance have been neglected in deriving it. The research in the present paper indicates that amplifications of peak internal pressure of 30% or more can occur (see Figs. 5, 8 and 10).

## 5. Conclusions

This paper considers the influence of the sizes of dominant wall opening and volume along with the approach wind speed, on internal pressure fluctuations. The outcomes of this study are applicable to analyzing internal pressure in buildings within a range of internal volumes and dominant opening sizes encountered in practice. Numerical methods were used to estimate fluctuating standard deviation and peak (i.e. design) internal pressures and compare these to limited full-scale internal pressure measurements. The influence of approach wind speed on fluctuating internal pressure is also assessed, and the design internal pressure coefficients for a range of opening and volume sizes, is presented in terms of the non dimensional opening size to volume parameter $S^* = (a_s/\bar{U}_h)^2(A^{3/2}/V_{Ie})$, for dominant wall openings with $\Phi_5 = \lambda_U/\sqrt{A}$ equal to 100, 50, 20 and 10. This study assumes that the air flow in and out of the opening in the envelope generates the well known Helmholtz resonance, which can amplify the internal pressure fluctuations compared to the external pressures at the opening.

This study showed that;

• The characteristics of the internal pressure fluctuations are significantly influenced by the size of the dominant opening and the size of the volume, and by the approach wind speed.

• The relationship between the internal pressure fluctuations and the external pressure at the dominant wall opening can be provided in terms of the standard deviation and peak pressure ratios versus $S^* = (a_s/\bar{U}_h)^2(A^{3/2}/V_{Ie})$, for a range of $\Phi_5$.

• The internal pressure fluctuations (standard deviation) are amplified over the external pressures at the dominant windward wall opening, when $S^*$ exceeds about 0.75.

• The $S^*$ at which the peak internal pressure is estimated to exceed the peak external pressure at the dominant windward wall opening, increases progressively with decreasing $\Phi_5$.

• The peak internal pressure can exceed these peak external pressures by 10% or more for $S^*$ greater than about 8.0

• The internal pressure fluctuations (standard deviation) are attenuated compared to the external pressures at the dominant windward wall opening for $S^*$ less than about 0.15. This attenuation increases with decreasing $\Phi_5$.

• The internal pressure peak factor $g_{pI}$ increases from 3.0 to more than 5.0 with increasing $S^*$.

• The relationships of internal pressure fluctuations resulting from a dominant leeward wall opening to external pressure fluctuations at the leeward wall opening have similar trends as for the building with a dominant windward wall opening.

• A simple reduction factor for large internal volumes that is always less than 1.0, as adopted in ASCE-7, cannot be justified.

• For wind-tunnel tests involving measurements of fluctuating internal pressures, internal volumes should be scaled correctly to ensure that the parameter $S^*$ has the same values in full- and model-scale. This normally requires increase of the internal volumes from the values obtained by simple geometric scaling, as previously found by Holmes (1979, 2008).

## References

American Society of Civil Engineers (2005), *Minimum design loads for buildings and other structures*, ASCE 7-05, A.S.C.E., New York.

Ginger, J.D., Yeatts, B.B. and Mehta, K.C. (1995), "Internal pressures in a low-rise full-scale building", *Proc. 9th International Conference in Wind Engineering*, New Delhi, Vol 1 (1995) 512-523.

Ginger, J.D., Mehta, K.C. and Yeatts, B.B.(1997), "Internal pressures in a low-rise full scale building", *J. Wind Eng. Ind. Aerodyn*., **72**, 163-174.

Ginger, J.D. (2000), "Internal pressure and cladding net wind loads on full scale low-rise building", *ASCE Struct Eng,* **126**, 538-543.

Harris, R.I. (1990), "The propagation of internal pressures in buildings", *J. Wind Eng. Ind. Aerodyn*., **34**, 169-184.

Holmes, J.D. (1979), "Mean and fluctuating internal pressures induced by wind", *Proc. 5th Int. Conf. on Wind Eng*., Colorado USA, Vol. 1, pp. 435-450, Permagamon Press, Oxford, U.K.

Holmes, J.D. (2008), Discussion of : "Net pressures on the roof of a low-rise building with wall openings" by Sharma,R.N. and Richards, P.J., *J. Wind Eng Ind. Aerodyn*. **93**, 267-291, 2005, to appear 2008.

Kopp, G.A., Oh, J.H. and Inculet, D.R. (2008), "Wind induced internal pressure in houses", *ASCE J. Struct Eng*, **134**, 1129-1138.

Levitan, M.L. and Mehta, K.C. (1992), "Texas Tech field experiments for wind loads. Part II: Meteorological instrumentation and terrain parameters", *J. Wind Eng. Ind. Aerodyn.*, **43,** 1577-1588.

Liu, H. (1978), "Building code requirements on internal pressure", *3rd US Conference on Wind Engineering*, Gainesville, Florida, USA, VI-7.

Oh, J.H., Kopp, G.A.,Inculet, D.R. (2007), "The UWO contribution to the NIST aerodynamic database for wind loads on low buildings: Part 3. Internal pressures", *J. Wind Eng. Ind. Aerodyn.*, **95**, 755-779.

Sharma, R.N. and P. J. Richards, P.J. (2003), "The influence of Helmholtz resonance on internal pressures in a low-rise building", *J. Wind Eng. Ind. Aerodyn.,* **91,** 807-828

Shi-ce, Yu Wen-juan, Lou and Bing-nan, Sun (2006), "Wind-induced internal pressure fluctuations of structure with single windward opening", *J. Zhejiang University, Science* A,**7** (3), 415-423

Standards Australia, (2002),. *Structural design actions. Part 2: Wind actions*. Australian/New Zealand Standard AS/NZS 1170.2:2002.

Vickery, B.J. (1994), "Internal pressures and interactions with the building envelope", *J. Wind Eng. Ind. Aerodyn.*, **53** 125-144

*CC*